ENSTA Bretagne
Ifremer
15ÈMES JOURNÉES DE L'HYDRODYNAMIQUE
22 - 24 novembre 2016 - Brest

A 3D Visualization of the Bubble Sweep-down Phenomenon around two Ship Bow Models

Visualisation 3D du phénomène de bullage autour de deux modèles d'étraves

B. MALLAT*, G. GERMAIN*, J.Y. BILLARD†
B. GAURIER*, J.V. FACQ*, T. BACCHETTI*

* IFREMER, Laboratoire Comportement des Structures en Mer
150 Quai Gambetta, 62200 Boulogne sur mer
† IRENAV, Ecole Navale
CC 600 - Lanveoc F-29240 BREST Cedex 9
bkhaddaj@ifremer.fr

Summary

The bubble sweep-down phenomenon around oceanographic research vessels generates acoustic disturbances. This phenomenon has affected the acoustic surveys for many years and is still a significant issue. The reason is that neither towing tank trials nor numerical simulations are able to properly address this phenomenon. We proposed a specific experimental protocol in a wave and current circulating tank allowing a 3D visualization of the bubble sweep-down phenomenon around two ship models with different bow geometries. Visualisations and Particle Image Velocimetry (PIV) measurement results both obtained in the bow vicinity of the two ship models are presented in this paper. These results allow a better representation of the phenomenon compare to previous results obtained only in 2D planes.

Résumé

Le phénomène de génération de bulles autour des navires de recherche océanographique génère des perturbations acoustiques. Ce phénomène affecte les relevés acoustiques depuis de nombreuses années et constitue toujours une problématique importante. La raison est que ni les essais en bassin de traction, ni les simulations numériques sont en mesure de traiter correctement ce phénomène. Nous proposons un protocole expérimental spécifique dans un bassin de circulation à houle et courant permettant une visualisation 3D du phénomène de bullage autour de deux modèles de navires avec différentes géométries d'étraves. Les résultats de visualisation du phénomène ainsi que des mesures par PIV autour des deux modèles d'étraves sont présentés dans ce papier. Ces résultats permettent d'obtenir une meilleure description du phénomène d'aération comparée avec des résultats obtenus précédemment dans un plan 2D.

I – Introduction

The bubble sweep-down phenomenon is a widely well known phenomenon that has been experienced to some degree on nearly every research vessel. It has detrimental effects on scientific sonar systems. The causes are less widely understood. On many specialized vessels, such as oceanographic survey and research vessels, warships and fisheries survey outfitted with underwater acoustic transducers, bubble-sweep down can significantly degrade the effectiveness of transducer performance. This phenomenon is separated into two important events : the first one is the formation of bubbles by breaking waves coming from natural wind or the bow entry into the water, and the second one is the training of these bubbles by a path backwards along the ship hull and under the transducers which disrupt the acoustic signals and may result to a considerable reduction of the ships productivity.

This phenomenon has affected the acoustic surveys for many years [1] and is still a significant issue [2,3]. The reason is that neither towing tank trials nor numerical simulations [4] are able to properly address this phenomenon [5]. Despite all these studies, the experimental characterization of bubble generation by the breaking bow waves of a ship are limited. The behaviour of these waves, depending on the bow geometry and the Froude number, have been well studied by [6], [7] and [8]. However studies of bubble generation in this configuration are scarse. Thus, this non-trivial phenomenon requires the development of a specific methodology to better study it.

As far as the diphasic problem is extremely difficult to handle properly with the common tools, a specific experimental protocol has been developed in a circulating tank, allowing the visualization of bubbles generation around a specific ship bow [9]. This protocol is based on the simulation of conditions under which bubble sweep-down can be observed at full scale. In this study [9], the bubble sweep-down phenomenon has been investigated in 2D dimensions on a plane illuminated by a vertical laser sheet near the bow of the ship. Occurrence frequency of bubble clouds, bubble dynamics in terms of area, depth and vertical velocity and PIV data analysis have been performed in this plane allowing a great characterization of the phenomenon [10]. However, it is well known that this study is still limited because of the complexity of this phenomenon that occurs in 3 dimensions. Thus, a development of an experimental set-up allowing to identify where these bubbles detected under a 2D study are really located in depth of field is an important issue to obtain a 3D knowledge of the bubble sweep-down phenomenon. Are these bubbles located in the 2D plane, in front of the plane or behind the plane ?

The objective of this work is to present an experimental protocol that we recently conducted allowing a 3D visualization of the bubble sweep-down phenomenon around two ship models with different bow geometries under the same experimental protocol. The first part of this paper presents the experimental set-up allowing the reproduction of the phenomenon in the flume tank. The video system used to characterize the flow is then described. The second part of this paper is devoted to the visualization of bubble clouds around the two models from different points of view. The final part of this paper focuses on PIV data analysis in the bow vicinity of the classic bow of Pp ? and the inverted bow to highlight the behaviour of the breaking wave during a wave period with and without bubbles.

II – Experimental set-up

Experiments have been carried out at the Ifremer (French Research Institute for Exploration and Exploitation of the Sea) wave and current flume tank (Figure 1). The tank working section is 18m long by 4m wide and 2m deep. The streamwise flow velocity range is U=0.1 to 2.2m/s. A wave generator (Figure 2) generates regular and irregular waves with a frequency range between f = 0.5 and 2Hz and a maximum amplitude of A = 300mm with a current speed up to 0.8m/s. It can be easily moved between an upstream or a downstream surface position to create waves propagating with or against the current. Measurements revealed that the resulting reflection coefficient is lower than 12% for all the usual frequencies and amplitudes. A side observation window of $8 * 2m^2$ placed on one side of the tank allows users to observe the behavior of the ship model during trials. In such facility and unlike towing tanks where models are free to heave and pitch, the model has been fixed on a motion generator system (hexapod) able to generate all kinds of motions. The free surface elevation has been measured by wave gauges placed upstream the ship bow.

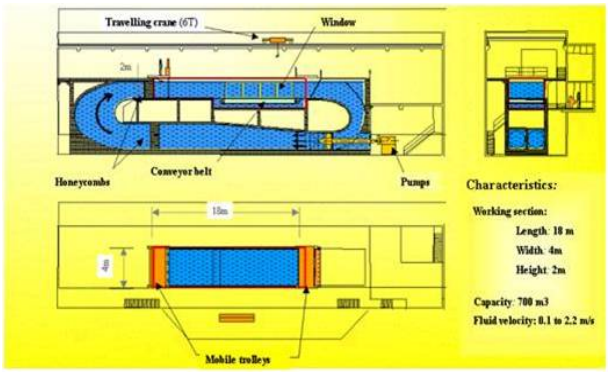

FIGURE 1 – Schematic view of the wave and current circulating tank.

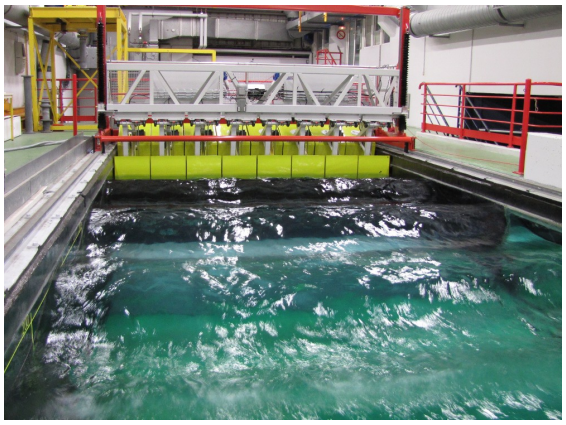

FIGURE 2 – View of the wave generator system with regular waves and current.

To reproduce the bubble sweep-down phenomenon observed on the French oceanographic research vessel Pp ? during the acoustic survey Essbulles performed in 2005 [8], a 1/30 scale ship model has been considered. The main conditions during this survey are : a ship speed of 8 knots, a wavelength of 109m, a significant wave height Hs of 2.8m, and a wave period Tp of 8.4s. To reproduce navigation conditions and sea state encountered during the sea survey and regarding the Froude similitude (Fr = $V^2/g.Lpp$ where V is the

ship speed, g is the gravity and Lpp is model length), the flow velocity in the flume tank is fixed at 0.75m/s and the wave amplitude at 33mm with a frequency of 0.85Hz.

Tests have been conducted on two 1/30 scale ship models with different bow geometries to study the effect of the bow geometry on the bubble sweep-down phenomenon. The first model is a classic bow of the oceanographic research ship Pourquoi pas ? (Pp ?). The second one is an inverted bow designed in a manner to maintain the overall length, width and draft of the Pp ?. The total drag (residual and skin friction drag) is lowered by 10% comparing with the classic bow. It has been designed at a scale of 1/30, that corresponds to a ship model of 3.13m length between perpendiculars (Lpp), 0,67m beam and 0.182m draft. Figure 3 presents the two models with a side and front views. Trials have been conducted on the front part only (1/3 of the model) to avoid perturbations coming from the model stern.

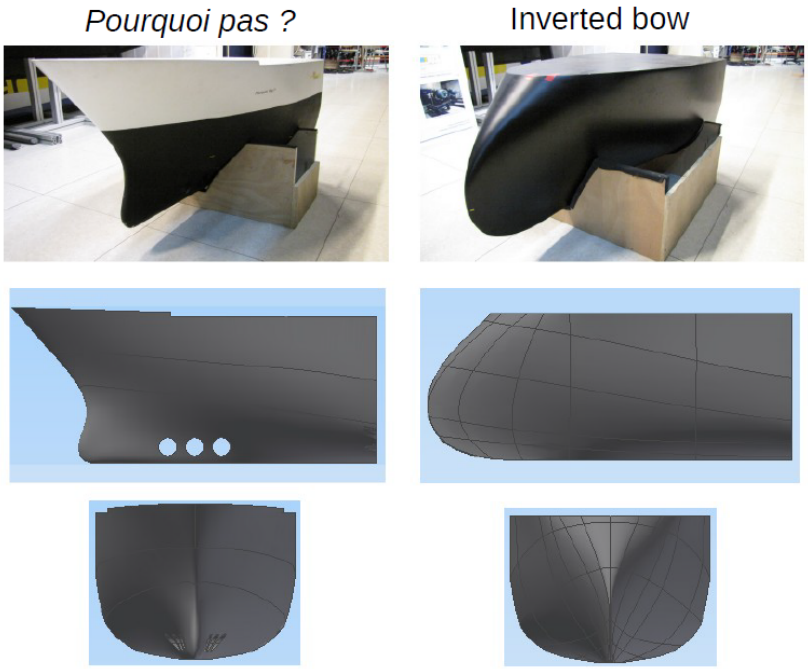

FIGURE 3 – View of the two 1/30 scale ship models.

Figure 4 presents the locations of instrumentations used in this study : the three cameras, the laser sheet and the wave gauges.

Two-dimensional time-resolved PIV measurements have been carried out with the cam1 located at the bottom of the tank. The focal lens of this camera is 20mm with a 1600x1200 $pixels^2$ resolution. Silver-coated glass particles of $10\mu m$ diameter have been used to seed the tank. Illumination has been provided horizontally by a standard, frequency-doubled, double-cavity Nd :YAG laser with a pulse energy of 120mJ per pulse using an excitation wavelength of 532nm. The time between pulses is fixed to t=$800\mu s$. The camera (Hi-sense CCD camera) recording PIV images has a 8.5Hz frequency for a double-frame images to obtain 10 velocity maps per wave period. The distance between the camera 1 and the laser sheet is 1.6m ; the camera is located perpendicularly to the laser sheet. DynamicStudio software from Dantec Dynamics has been used for PIV image processing. Instantaneous velocity vector fields have been obtained using an adaptive correlation PIV algorithm with an interrogation window size of 16x16 $pixels^2$ and a non-overlapped adjacent window. The physical dimension of the PIV plane is $621.1 * 461.1 mm^2$. We have to

note that PIV velocity maps in this case are not fully representative of the flow because of lot of surface reflections. However, these PIV data analysis give a good approximation and representation of the angle evolution between the bow and the breaking wave. That allow us to better characterize the surface behaviour when bubble clouds occur or not as we could see after.

Two other cameras have been disposed around the ship model (Figure 4) in order to characterize and quantify the propagation of air bubbles around the ship bow from different views. The first one (cam2) is installed above the free surface allowing to visualize the breaking wave phenomenon with an approximate physical dimension plane of $512 * 384mm^2$ and a focal lens of 25mm. The second one (cam3) is located behind the side flume tank observation window allowing the visualization of air bubbles propagating along the ship hull. The physical dimension plane of the cam3 is $635 * 476mm^2$ and the focal lens is 60mm. All cameras have been synchronized with the same PIV system.

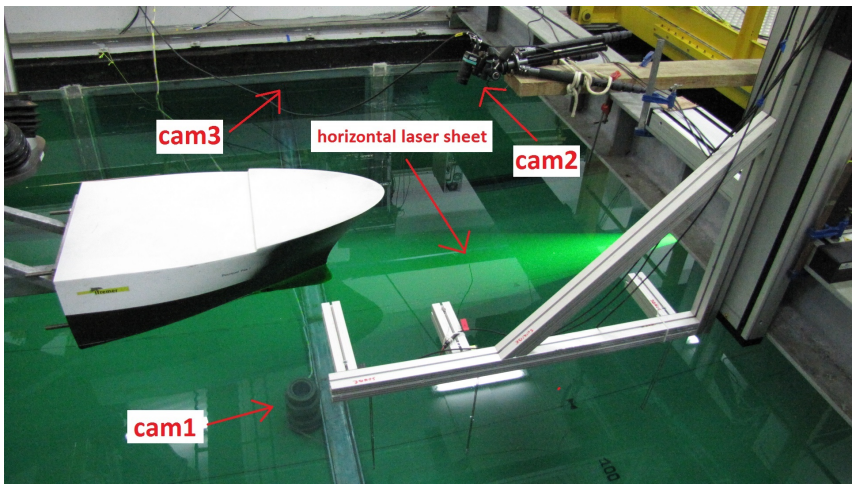

FIGURE 4 – View of the experimental set-up : locations of the three cameras, the laser sheet and the wave gauges.

III – Results and discussions

As mentioned above, previous studies have been done to characterize the bubble sweep-down phenomenon in 2 dimensions. In this case, illumination has been provided vertically on a plane in the bow vicinity of the ship bow (see figure 5) and images have been taken by a camera behind the observation window allowing the visualization and propagation of air bubbles along the ship hull. Figure 6 presents an example of an image taken in such experiments where a bubble cloud is generated. Occurrence frequency of bubble clouds, bubble cloud dynamics and PIV data analysis have been investigated. Bubble clouds have been detected on the raw images and analysed by a gray scale level in order to calculate in 2D the area, depth and velocity of this bubble cloud. However, all these results are performed in a plane without knowing bubble positions and if those bubbles are or not in the illuminated plane. For a 3D characterization, two cameras are mounted as we mention in the experimental set-up to visualize the bubble clouds from different points of view and illumination has been provided horizontally. Figures 7 and 8 show an exemple of a wave period with bubble generation taken by the three cameras around the classic bow of the Pp ? and the inverted bow respectively. From the camera at the bottom tank, we visualize the position of bubbles transversely in width. It is the main information that we had not

before in 2 dimensions study. With this information, we are now able to identify where bubbles shown from the side camera are located breadthwise thanks to the camera at the bottom of the tank. The camera above the bow allows a visualization of the free surface, we can identify the behaviour of this surface when a bubble cloud is generated around the two ship models : what is the amount of the breaking wave with and without bubbles, what is the angle between the breaking wave and the bow with and without bubbles ?.. From all these informations, we see that the phenomenon is 3D and it can not be completely described using only one set of images from one selected camera.

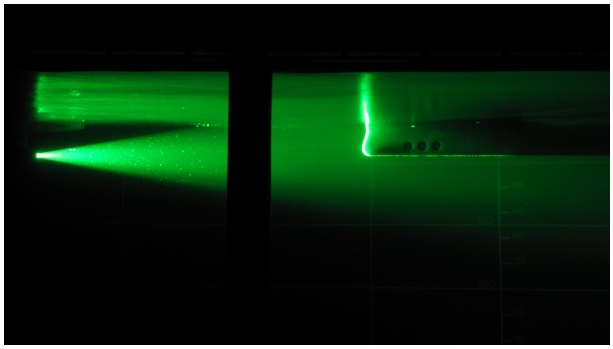

FIGURE 5 – The vertical laser sheet around the classic bow of Pp ? for PIV measurements.

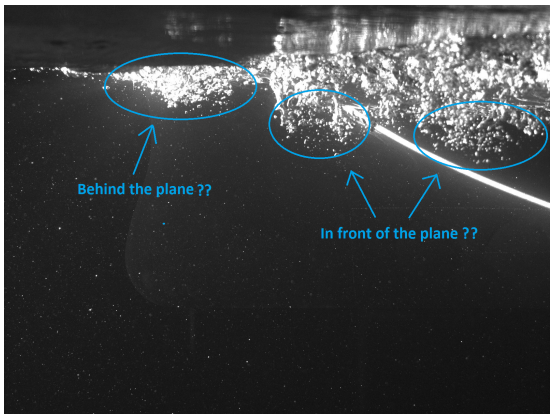

FIGURE 6 – A raw image with bubble cloud around the classic bow of Pp ? in the 2 dimensions study.

Regarding the comparaison between the two ship models, we can see from the images of cam3 that the bubble cloud generated around the classic bow of the Pp ? is more energetic in terms of area and depth than the bubble cloud generated around the inverted bow. Images from cam1 and 2 show that the breaking waves around the classic bow of the Pp ? take place at the front of the bow allowing to generate bubbles away from the bow. It is not the case for the inverted bow where the breaking waves are less energetic. Images from cam2 above the free surface show a greater angle evolution of breaking wave around the classic bow of the Pp ? comparing to the inverted bow. All these observations are related to the bow geometrie. The fact that we have much lower energetic breaking waves around the inverted bow comparing to the Pp ? comes from the interaction between the incoming wave and the bow shape. There is a great difference of the bow geometries for both ship models. The flairing of the bow of the Pp ? is the origin of a high reflection of the incoming wave at the bow allowing to generate energetic breaking waves and consequently more bubbles tending to go further in depth.

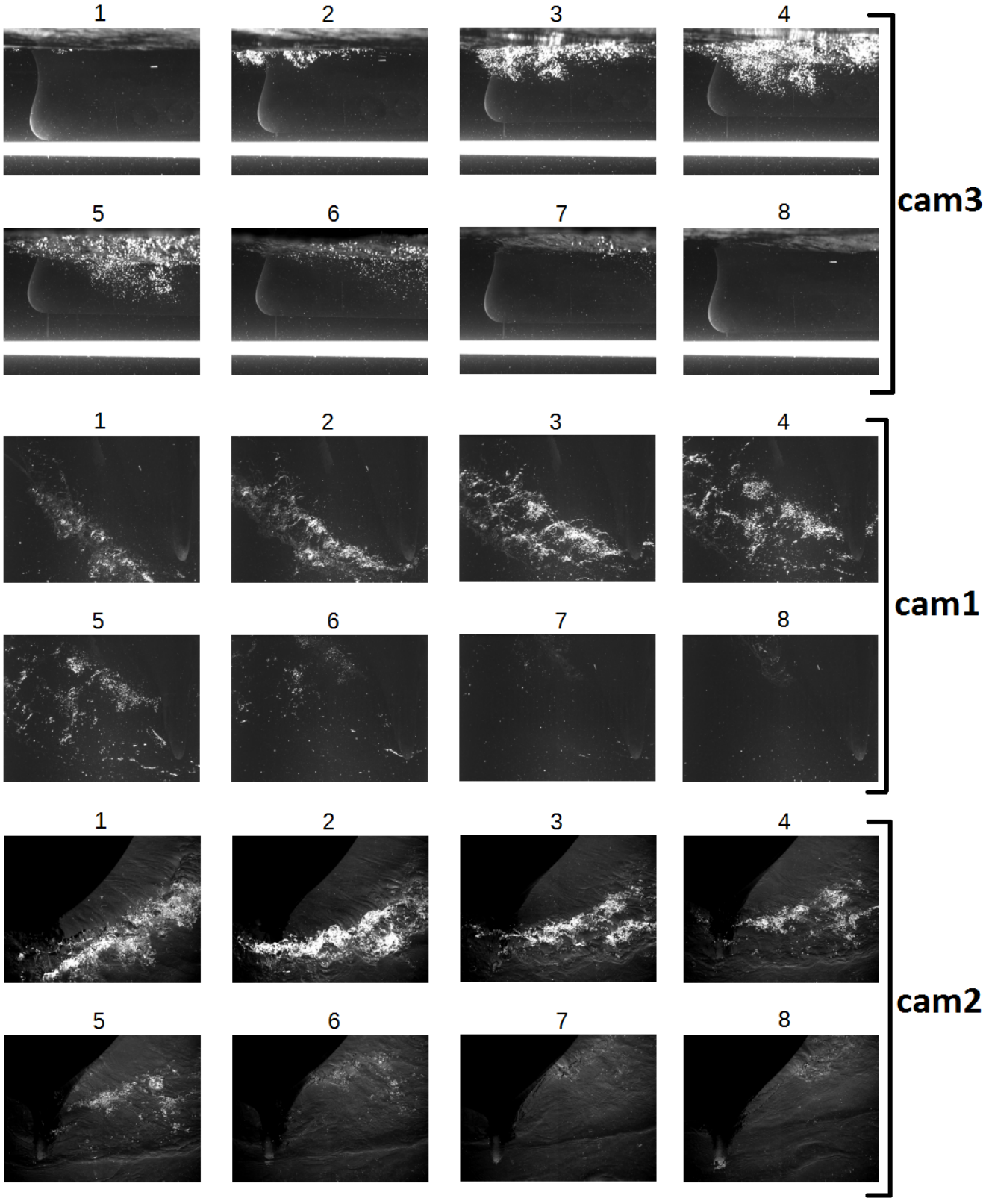

FIGURE 7 – Images taken by the three cameras during a wave period with bubbles around the classic bow of Pp ?.

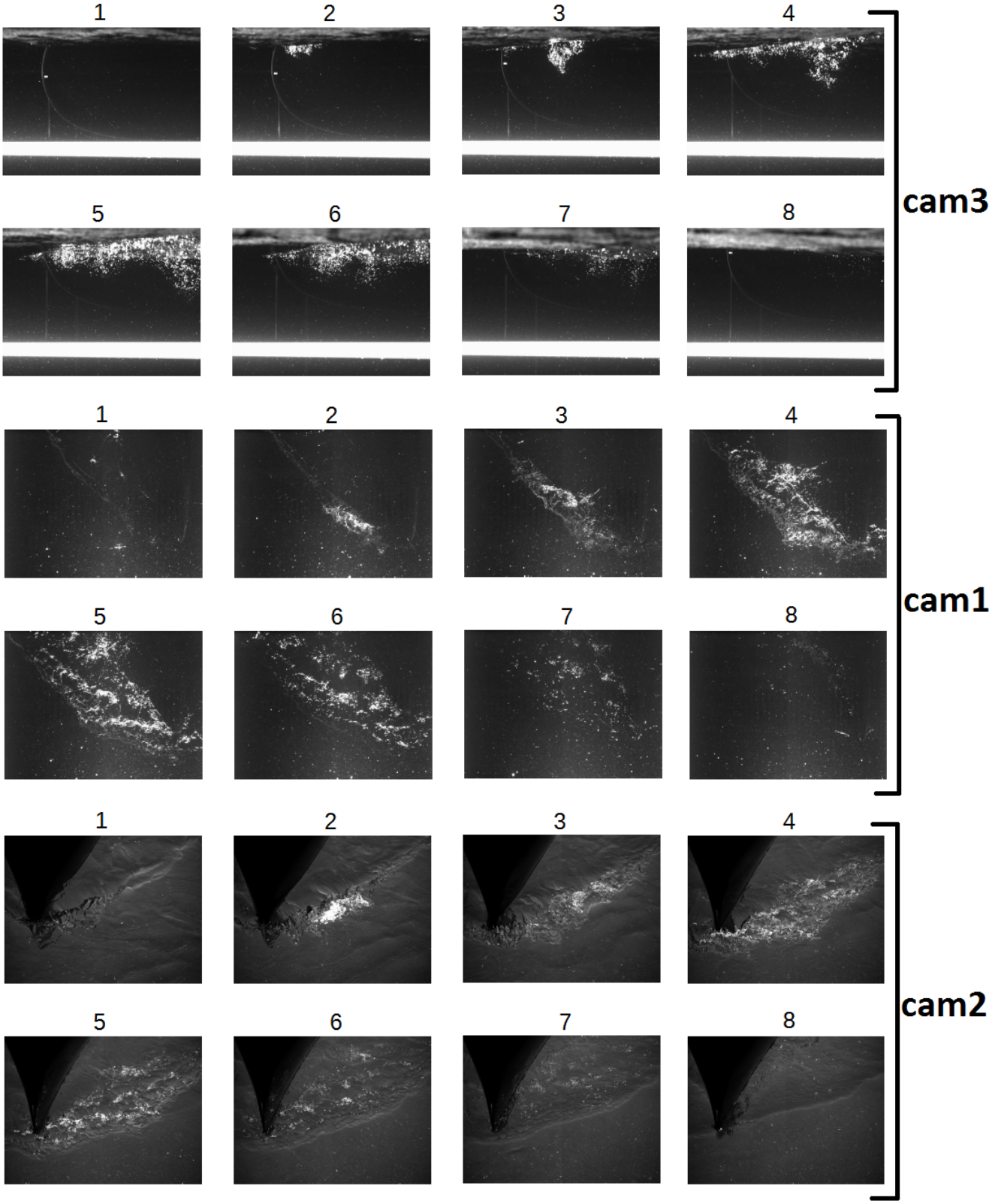

FIGURE 8 – Images taken by the three cameras during a wave period with bubbles around the inverted bow.

Figures 9 and 11 present image sequences taken by the three cameras during a wave period without and with bubbles respectively around the classic bow of the Pp ?. The PIV data analysis corresponds to the instantaneous velocity vector field of each raw image from 1 to 9 of the cam1. Each image from 1 to 9 corresponds to the phase locations given in Figure 10. The red line shows the angle evolution between the breaking wave and the bow. We can see that this angle reaches a value of nearly 63° during the wave period without bubbles (Figure 9). There is not a breaking wave angle trace before the phase 5. During the wave period with bubbles (Figure 11), we can see that the breaking wave take place and begin at the front of the bow making a great angle that reaches nearly 90° after the wave peak when bubbles are generated and then propagated along the ship hull. The breaking wave angle trace starts from phase 1. The angle evolution during a wave period with bubbles is more important, especially after the wave peak in phase 5 to the breaking wave phenomenon that generate bubbles until phase 9. Regarding the comparaison between the classic bow of the Pp ? and the inverted bow during a wave period with bubbles, we can see that the evolution angle around the inverted bow (Figure 12) is less important and reaches a value of about 60°. The bow geometry effects are the main reason of this observation. The interaction between the incoming waves and the bow shape is different between the two ship models. There is a low reflection of the incoming waves at the inverted bow allowing to generate less energetic breaking waves not tending to get to the front of the bow as in the case of the classic bow of the Pp ?, reason why this angle is less important.

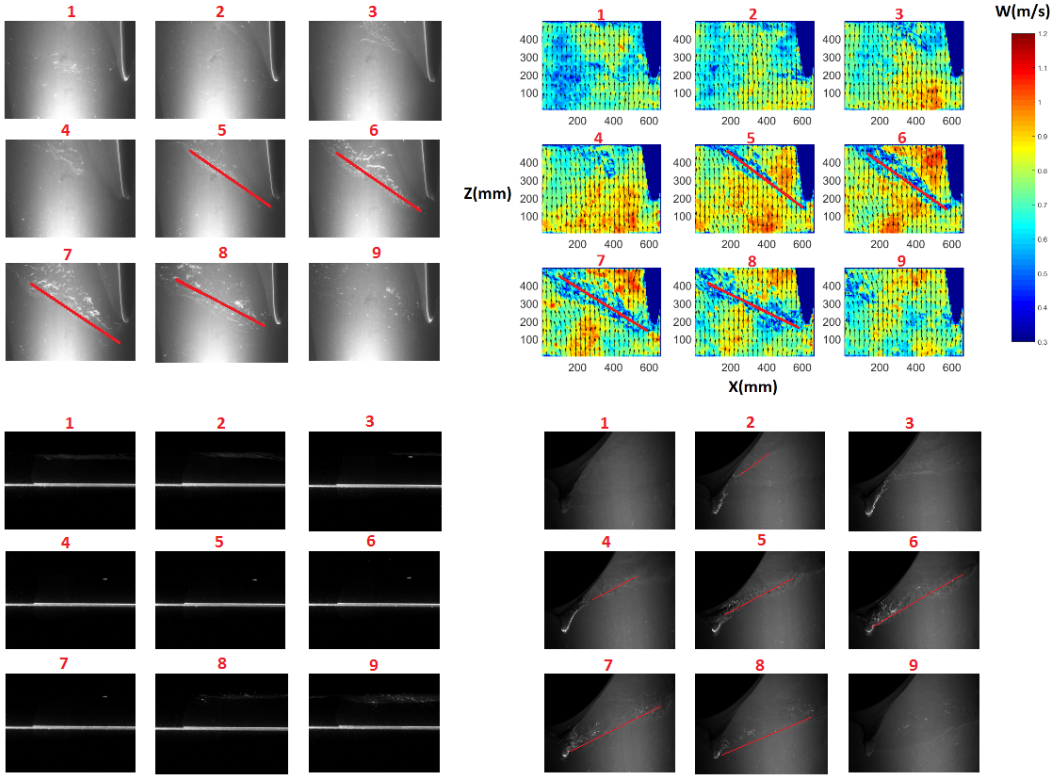

FIGURE 9 – Images taken by the 3 cameras. Each group of 9 graphs corresponds to nine consecutive instants of a same wave period **without bubbles** in the configuration with current, waves and motions around the **classic bow of Pp ?**. The image 5 corresponds to the wave peak at the bow. Top-left : images taken by cam1. Top-right : instantaneous vertical velocity vector fields of the images taken by cam1. Bottom-left : images taken by cam3. Bottom-right : images taken by cam2.

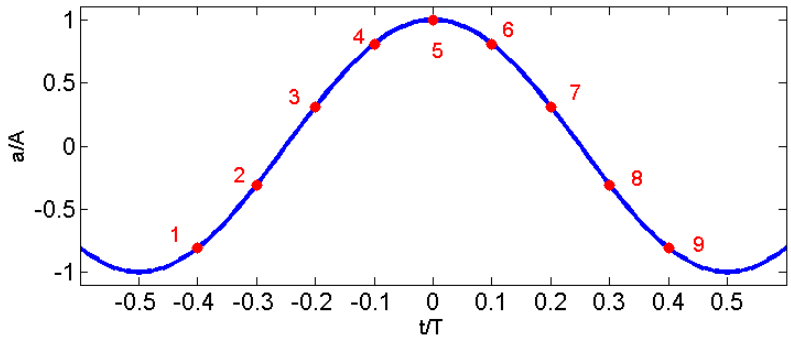

FIGURE 10 – Time evolution of the harmonic wave surface and the corresponding instants to calculate the phase average.

We recall that the PIV data analysis in this configuration is not really representative of the velocity maps. In other terms, PIV results give informations contained on two different planes : when breaking waves appear, the free surface is disturbed and induced reflections in the breaking wave zone. Thus, the flow velocities determined is wrong in this area. However, the obtained results give us a good representation of the angle of evolution of the breaking wave. On the other side, we obtain the current velocity of 0.75m/s away from the breaking wave area where the free surface is not disturbed and the PIV velocities are really the velocities in the laser sheet 230mm below the free surface.

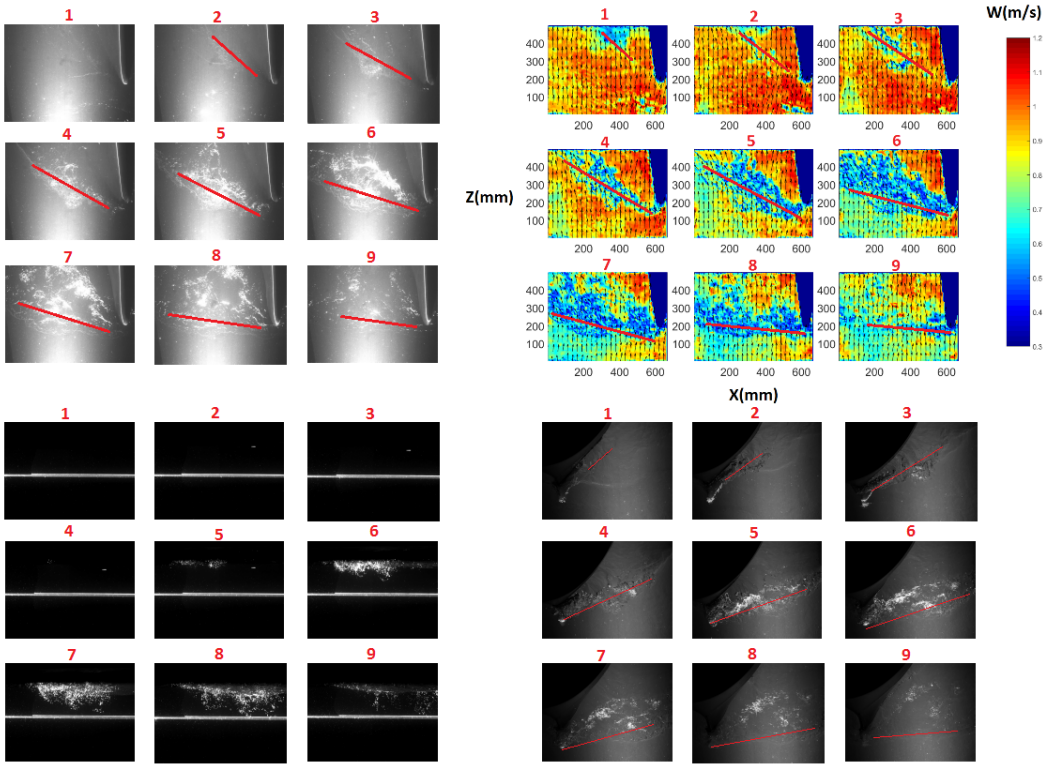

FIGURE 11 – Images taken by the 3 cameras. Each group of 9 graphs corresponds to nine consecutive instants of a same wave period **with bubbles** in the configuration with current, waves and motions around the **classic bow of Pp ?**. The image 5 corresponds to the wave peak at the bow. Top-left : images taken by cam1. Top-right : instantaneous vertical velocity vector fields of the images taken by cam1. Bottom-left : images taken by cam3. Bottom-right : images taken by cam2.

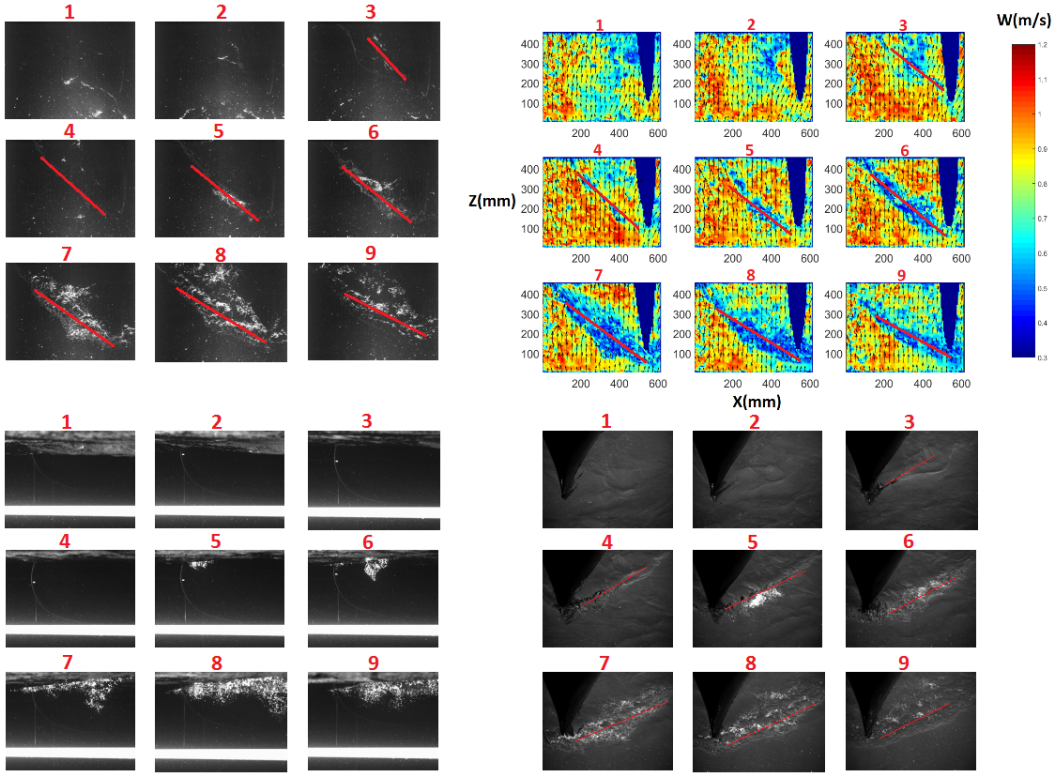

FIGURE 12 – Images taken by the 3 cameras. Each group of 9 graphs corresponds to nine consecutive instants of a same wave period **with bubbles** in the configuration with current, waves and motions around the **inverted bow**. The image 5 corresponds to the wave peak at the bow. Top-left : images taken by cam1. Top-right : instantaneous vertical velocity vector fields of the images taken by cam1. Bottom-left : images taken by cam3. Bottom-right : images taken by cam2.

IV – Conclusions

An experimental study of the bubble sweep-down phenomenon around two 1/30 scale ship models have been carried out in a wave and current circulating tank allowing a 3D visualization of the phenomenon. Three synchronized cameras located around the ship bow with an horizontal laser sheet enabled to visualize the bubble sweep-down phenomenon from different points of view. The generation and propagation of bubbles around the ship hull, bubble positions in width and the angle evolution of the breaking wave are the main results obtained by this experimental set-up. This method allows a new global apprehension and visualization of the bubble sweep-down phenomenon around a ship bow compared to previous studies where it is too much hard to identify the bubble positions in depth of field and if the bubbles are or not in these planes. The 3D characterization of the bubble clouds will help for the analysis of 2D PIV measurements performed on different planes.

In this work, PIV measurements have been done for the camera located at the bottom of the tank. The data analysis give a good representation of the breaking wave behaviour along a wave period with and without bubbles even if this data analysis process is not really representative of the velocity maps of the flow around the bow. Breaking waves around the classic bow of the Pp ? take place at the front of the bow making a large angle with the bow that reaches 90° during a wave period with bubbles. It is not the case

during a wave period without bubbles where the angle between breaking waves and the bow reaches about 63°.

A comparaison between two 1/30 scale ship models with different bow geometries has also been done and the results show that we have more energetic breaking waves around the classic bow of the Pp ? comparing to the inverted bow. These energetic breaking waves allow to generate bubbles tending to go further in depth.

Future work involves detection and evolution of each bubble around the ship bow. If we are able to identify the position of the same bubble on the two cameras behind the observation window and at the bottom of the tank, we can delimite an evolution of bubble cloud volume along the ship hull and so a better 3D knowledge of the bubble sweep-down phenomenon.

Références

[1] J. Dalen, A. Lovik, 1981, The influence of wind-induced bubbles on echo integration surveys, J. Acoust.Soc. Am., Vol.69, 1653-1659.

[2] Delacroix S., Germain G., Berger L., Billard J-Y., 2016. Bubble sweep-down occurrence characterization on Research Vessels. Ocean Engineering 111, 34-42.

[3] F. W. Shabangu, E. Ona, D. Yemane, 2014, Measurements of acoustic attenuation at 38kHz by wind induced air bubbles with suggested correction factors for hull-mounted transducers, Fisheries research, Vol.151, 47-56.

[4] F.J. Moraga, P.M. Carrica, D.A. Drew, R.T. Lahey Jr, 2008, A sub-grid air entrainment model for breaking bow waves and naval surface ships. Computer & Fluids, 37 :281-298.

[5] J.P. Johansen, Full-scale two-phase flow measurements on Athena research vessel, PhD Thesis of university of IOWA, 2010.

[6] Noblesse F., Delhommeau G., Guilbaud M., Hendrix D., Yang C., 2008, Simple analytical relations for ship bow waves, Journal of Fluid Mechanics, Vol.600, 105-132.

[7] Noblesse F., Delhommeau G., Guilbaud M., Liu H., Wan D., Yang C., 2013, Ship bow waves, Journal of Hydrodynamics, Vol.25, 491-501.

[8] Delhommeau G., Guilbaud M., David L., Yang C., Noblesse F., 2009, Boundary between unsteady and overturning ship bow wave regimes, Vol.620, 167-175.

[9] Delacroix S., Germain G., Gaurier B., Billard J-Y., 2016. Experimental study of bubble sweep-down in wave and circulating tank. Part I - Experimental set-up and observed phenomena. Ocean Engineering 120, 78-87.

[10] Delacroix S., Germain G., Gaurier B., Billard J-Y., 2016. Experimental study of bubble sweep-down in wave and circulating tank. Part II - Bubble clouds characterization. Ocean Engineering 120, 88-99.